

**New topological  $\text{Co}_2(\text{BDC})_2(\text{DABCO})$  as highly active heterogeneous catalyst for amination  
of oxazoles via oxidative C-H/N-H couplings**

Thach N. Tu,<sup>a, b, †</sup> Khoa D. Nguyen,<sup>a, †</sup> Truong N. Nguyen,<sup>a</sup> Thanh Truong,<sup>a, \*</sup> and Nam T. S.

Phan<sup>a, \*</sup>

<sup>a</sup>Faculty of Chemical Engineering, HCMC University of Technology, VNU-HCM, 268 Ly Thuong Kiet, District 10, Ho Chi Minh City, Vietnam.

<sup>b</sup>Center for Molecular and NanoArchitecture (MANAR), VNU-HCM, Ho Chi Minh City 721337, Vietnam.

<sup>†</sup>These authors contributed equally.

\*To whom correspondence should be addressed: tvthanh@hcmut.edu.vn and ptsnam@hcmut.edu.vn

## Supporting Information

**Table S1. Investigate the affection of HCl to the formation of VNU-10**

$\text{Co}(\text{NO}_3)_2 \cdot 6\text{H}_2\text{O}$	0.015 M				
$\text{H}_2\text{BDC}$	0.027 M				
DABCO	0.03 M				
AcOH ( $\mu\text{L}$ )	200				
Amount HCl ( $\mu\text{L}$ )	0	1	2	3	4
Color of $\text{Co}(\text{NO}_3)_2 \cdot 6\text{H}_2\text{O}$ solution	Purple	Blue	Blue	Blue	Deep Blue

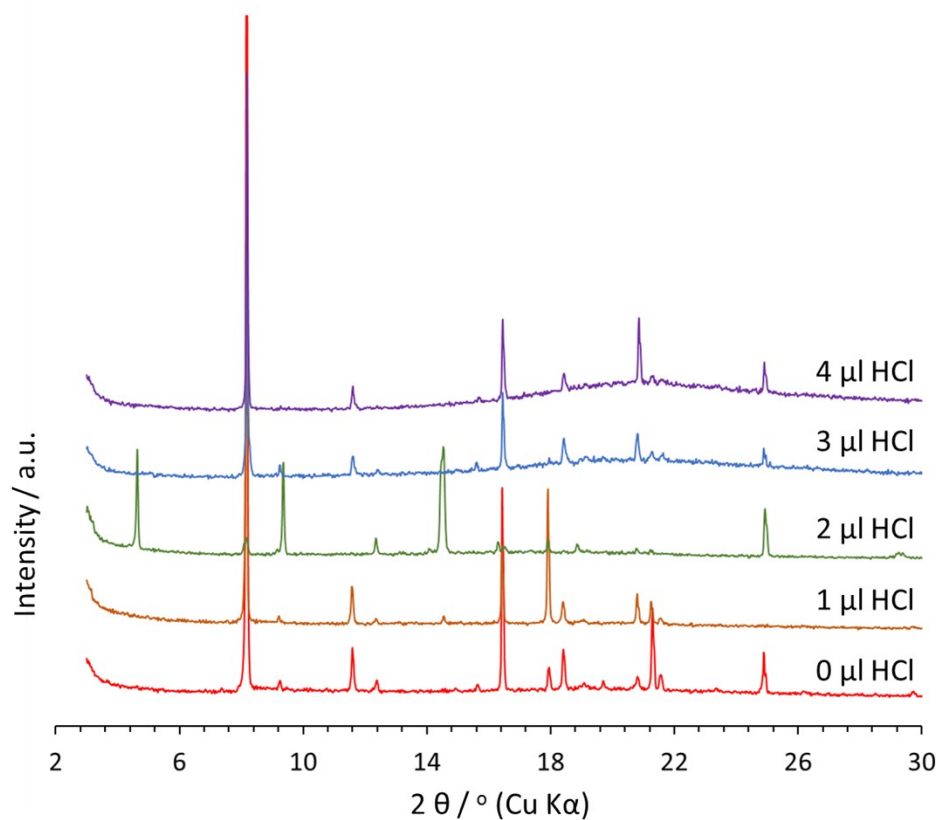


**Fig. S1** PXRD of obtained crystalline material at varied concentration of HCl

The investigated amount of HCl ranged from 0 to 4 μl, the amount of HCl, in which VNU-10 formed is 2 μl HCl.

**Table S2.** Investigate the affection of CH<sub>3</sub>COOH to the formation of VNU-10

Co(NO <sub>3</sub> ) <sub>2</sub> •6H <sub>2</sub> O	0.015 M									
H <sub>2</sub> BDC	0.027 M									
DABCO	0.03 M									
HCl (μl)	2									
AcOH (μl)	0	50	100	150	200	250	300	350	400	

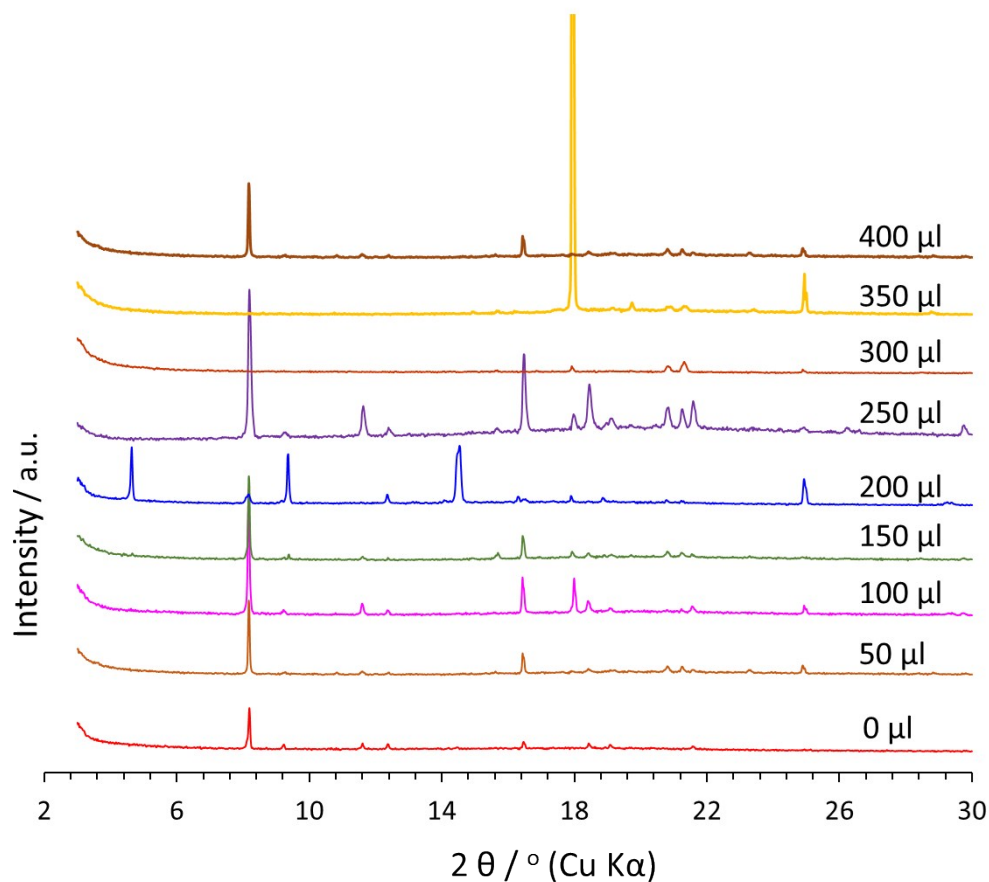


**Fig. S2** PXRD of obtained crystalline material at varied concentration of CH<sub>3</sub>COOH

The investigated amount of CH<sub>3</sub>COOH ranged from 0 to 400 μl, the amount of CH<sub>3</sub>COOH, in which VNU-10 formed is 200 μl CH<sub>3</sub>COOH.

### **Single Crystal Structure Determination of Co<sub>2</sub>(BDC)<sub>2</sub>(DABCO)**

Diffraction data set was collected at 100K on a Bruker APEX CCD diffractometer with CuKα radiation ( $\lambda = 1.54178 \text{ \AA}$ ). Bruker SMART program was used for data collection, and SAINT was used for cell refinement, and reduction. XPREP suggested a cubic space group P6/mmm. The structure was solved by direct methods and refined against all data using the shelxle program. Thermal parameters for all non-hydrogen atoms were refined anisotropically except the free water

molecule in pore volume. Introduction EXTI was used to refine again the highly disordered solvent molecules in the pores.

Table S3. Crystal data and structure refinement for VNU-10

Identification code	VNU-10	VNU-10 with SQUEEZE
Empirical formula	C <sub>11</sub> H <sub>10</sub> NO <sub>11</sub> Co	C <sub>11</sub> H <sub>10</sub> NO <sub>4</sub> Co
Formula weight	391	279
Temperature (K)	100(2)	
Wavelength (Å)	1.54178	
Crystal system	Hexagonal	
Space group	p6/mmm	
Unit cell dimensions	a = 21.5645(7) Å b = 21.5645(7) Å c = 9.4379(3) Å	α= 90.00 °. β= 90.00 °. γ= 120.00 °.
Volume (Å <sup>3</sup> )	3800.9(2)	
Z	6	
Density (calculated) (g/cm <sup>3</sup> )	1.028	0.732
Absorption coefficient (mm <sup>-1</sup> )	5.672	5.333
F(000)	1191	852
Crystal size (mm <sup>3</sup> )	0.2 × 0.04 × 0.04	
Theta range for data collection	2.37 ° to 65.1 °.	
Index ranges	-21 ≤ h ≤ 25; -25 ≤ k ≤ 25; -11 ≤ l ≤ 11	
Reflections collected	25049	
Independent reflections	1315 [R(int) = 0.1420]	1315 [R(int) = 0.1279]
Completeness to theta = 65.15°	0.999	
Absorption correction	multi-scan	

Refinement method	Full-matrix least-squares on F <sup>2</sup>	
Data / restraints / parameters	25049 / 2 / 101	25049 / 2 / 55
Goodness-of-fit on F <sup>2</sup>	1.123	1.115
Final R indices [ $I > 2\sigma(I)$ ]	R1 = 0.0868, wR2 = 0.2402	R1 = 0.0524, wR2 = 0.1480
R indices (all data)	R1 = 0.1010, wR2 = 0.2533	R1 = 0.0644, wR2 = 0.1551
Largest diff. peak and hole ( $e \cdot \text{\AA}^{-3}$ )	0.831 and -0.321	0.365 and -1.171

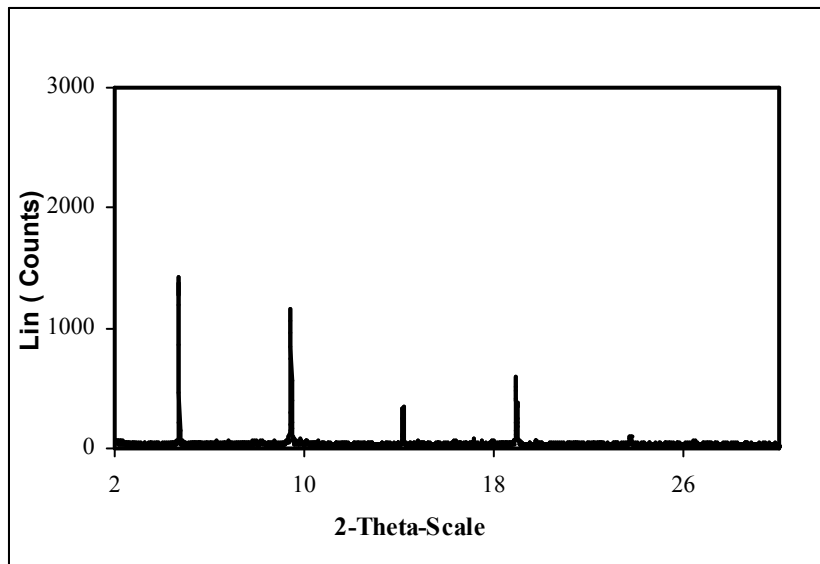


Fig. S3. X-ray powder diffractograms of the VNU-10

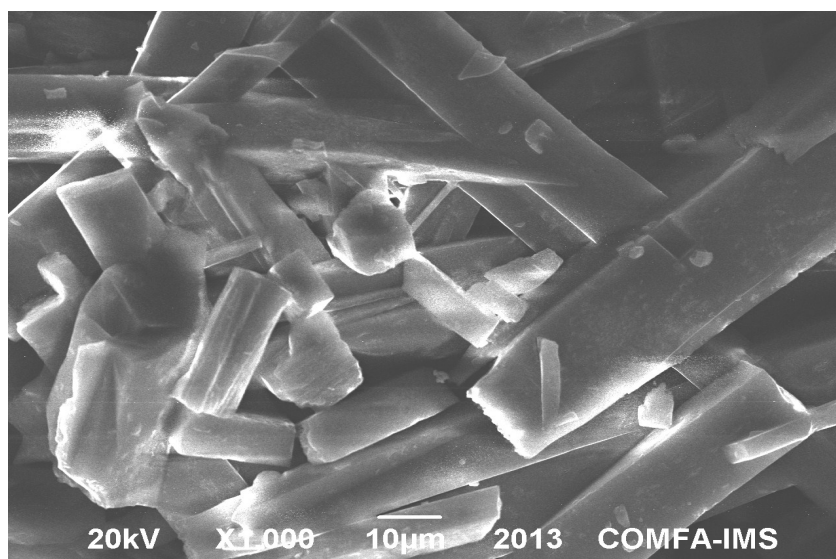


Fig. S4. SEM micrograph of the VNU-10

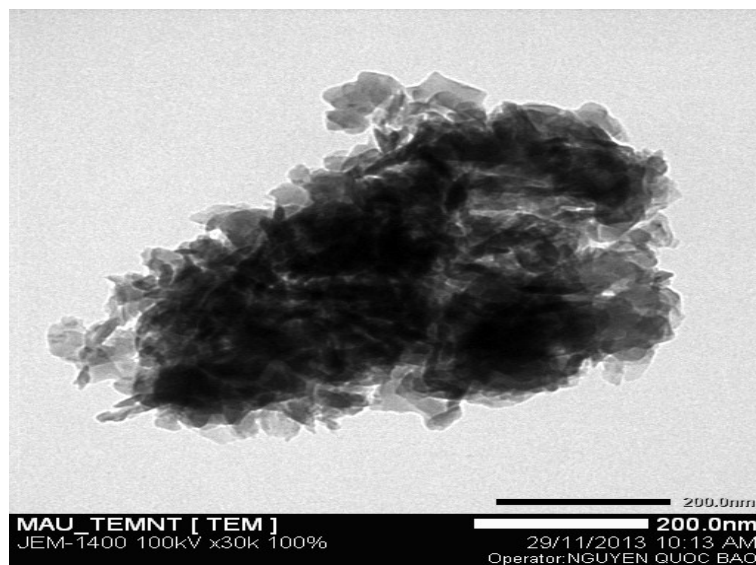


Fig. S5. TEM micrograph of the VNU-10

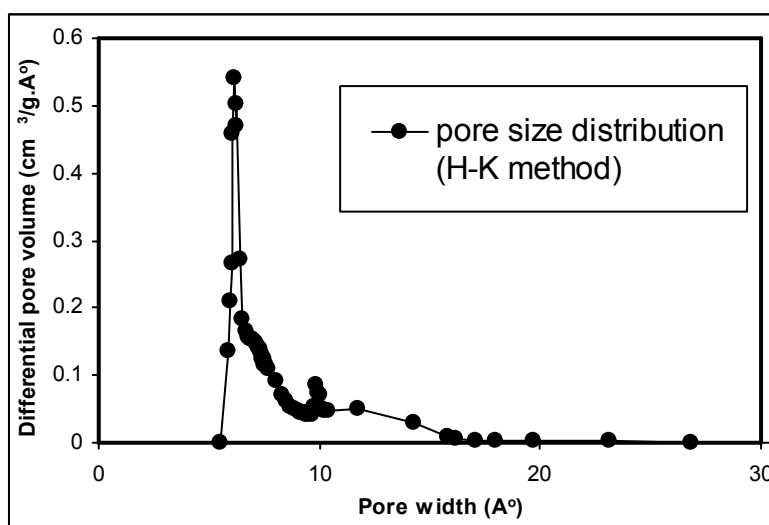


Fig. S6. Pore size distribution of the VNU-10

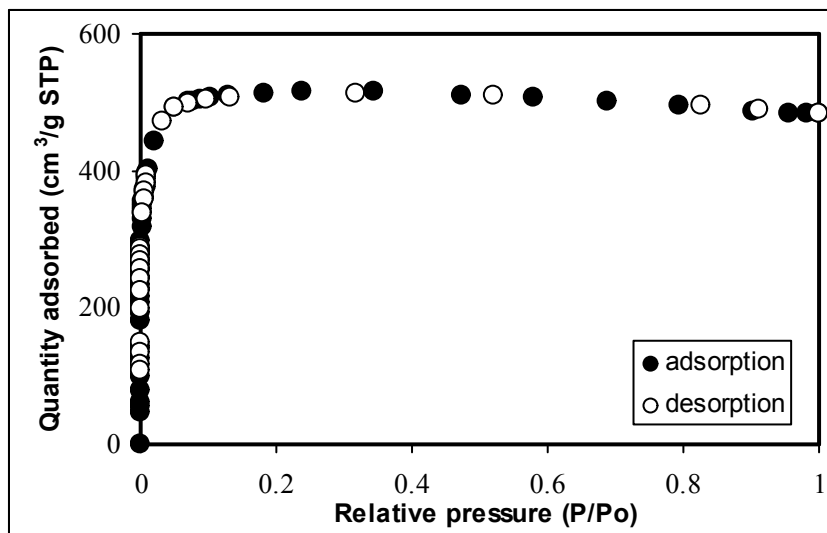


Fig. S7. Nitrogen adsorption/desorption isotherm of the VNU-10. Adsorption data are shown as closed circles and desorption data as open circles.

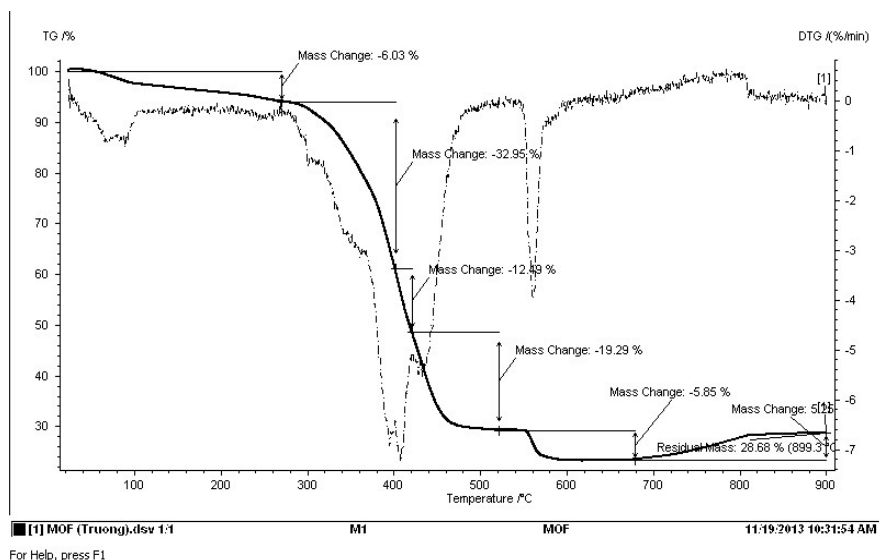


Fig. S8. TGA analysis of the VNU-10.



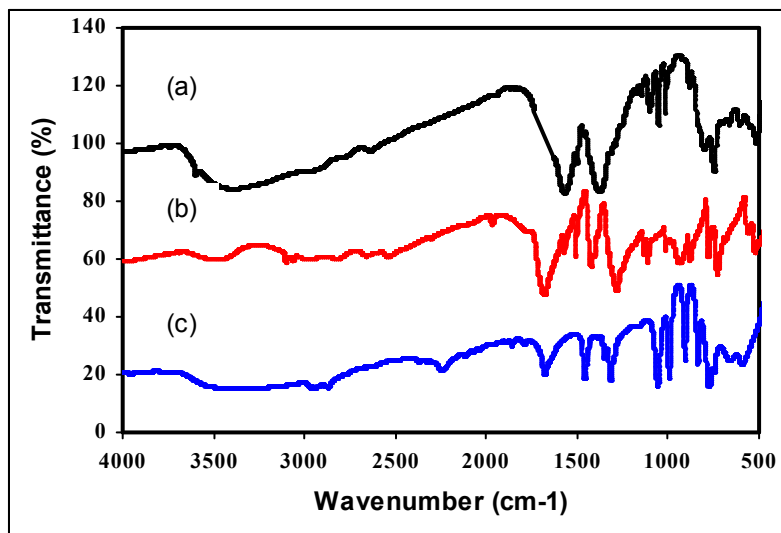


Fig. S9. FT-IR spectra of the VNU-10 (a), the 1,4-benzenedicarboxylic acid (b), and the 1,4-diazabicyclo[2.2.2]octane (c).

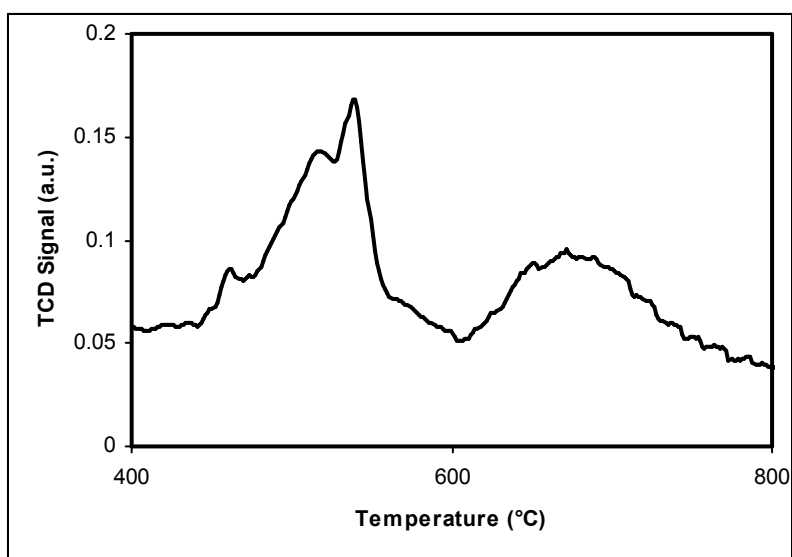


Fig. S10. H<sub>2</sub>-TPR profile of the VNU-10.

Elemental Analysis: Calcd. for  $\text{Co}_2\text{C}_{22}\text{H}_{26}\text{O}_{11}\text{N}_2 = [\text{Co}_2(\text{BDC})_2(\text{DABCO})] \cdot 3\text{H}_2\text{O}$ : C, 43.15; H, 4.28; N, 4.58%. Found: C, 43.19; H, 4.35; N, 4.50%.

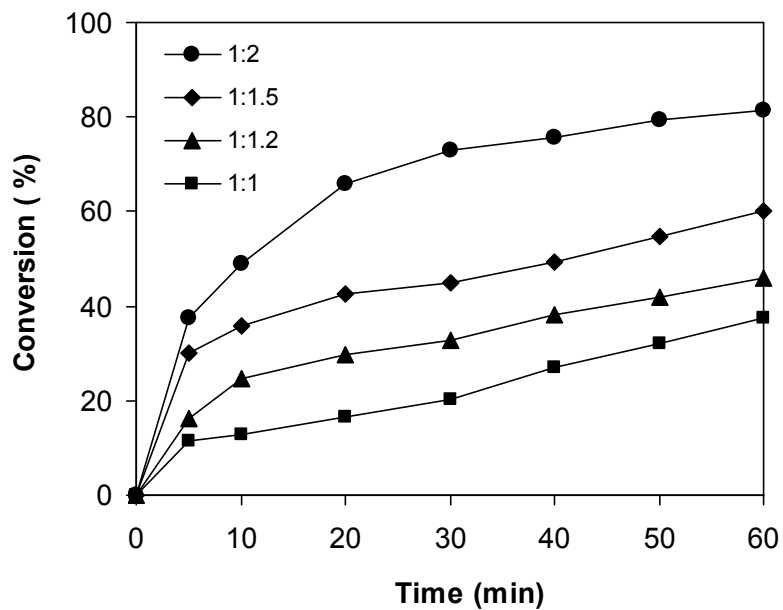


Fig.S11. Effect of benzoxazole:piperidine molar ratio on reaction conversion.

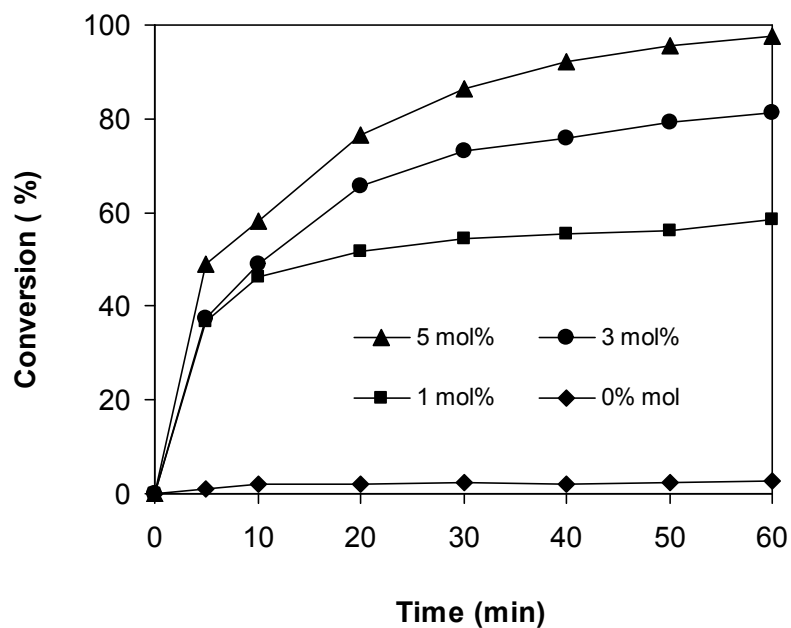


Fig. S12. Effect of catalyst concentration on reaction conversion.

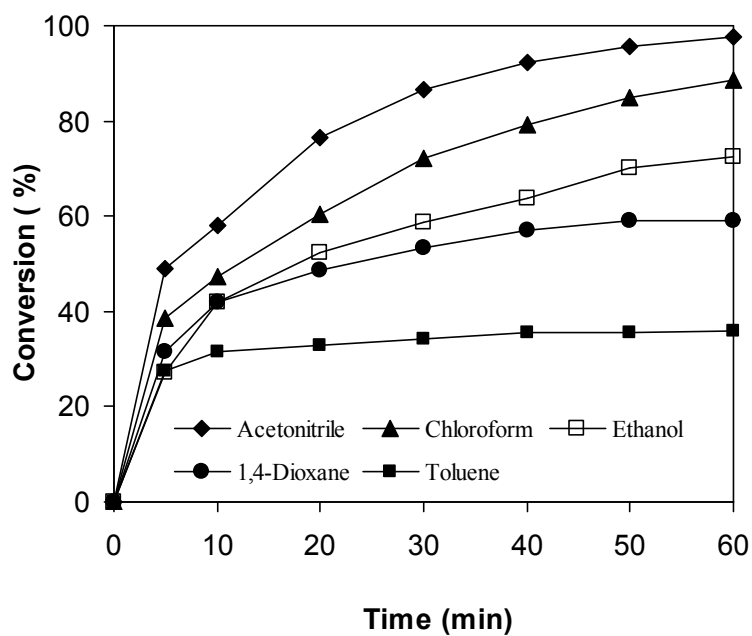


Fig. S13. Effect of different solvents on reaction conversion.

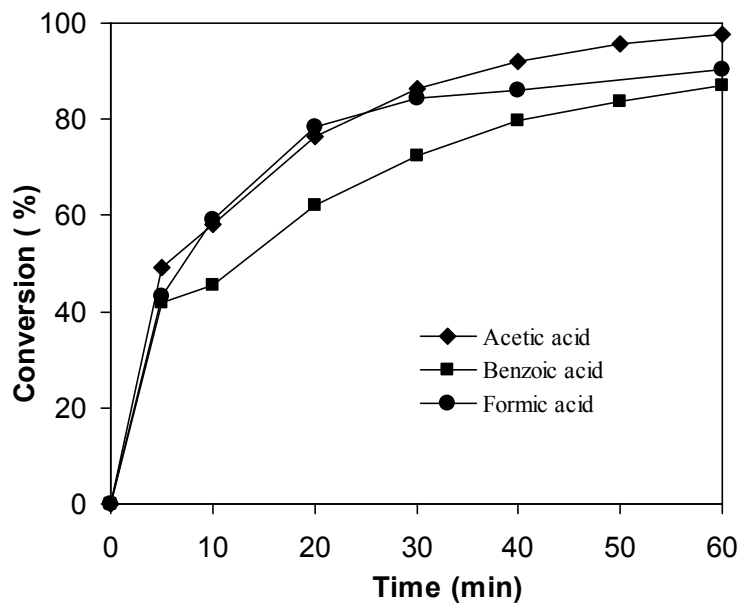


Fig. S14. Effect of different carboxylic acids on reaction conversion.

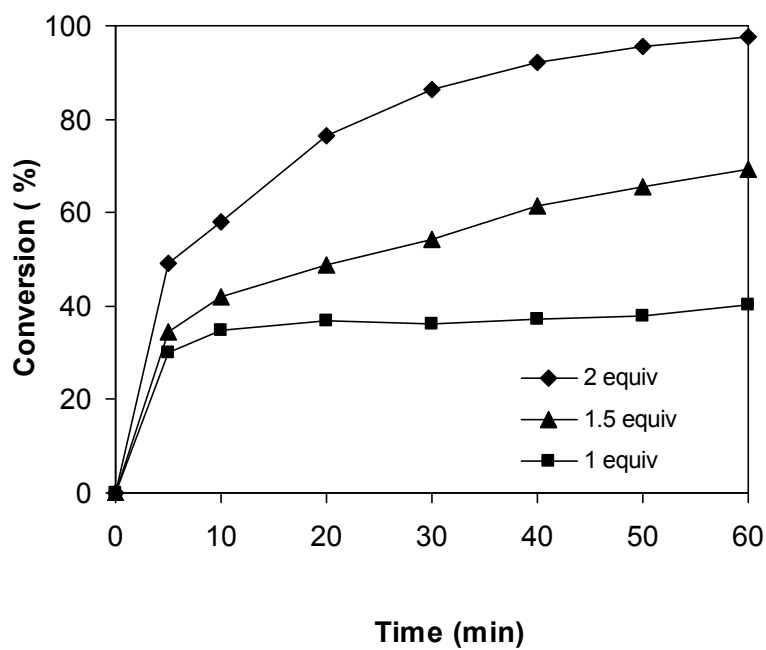


Fig. S15. Effect of acetic acid concentration on reaction conversion.

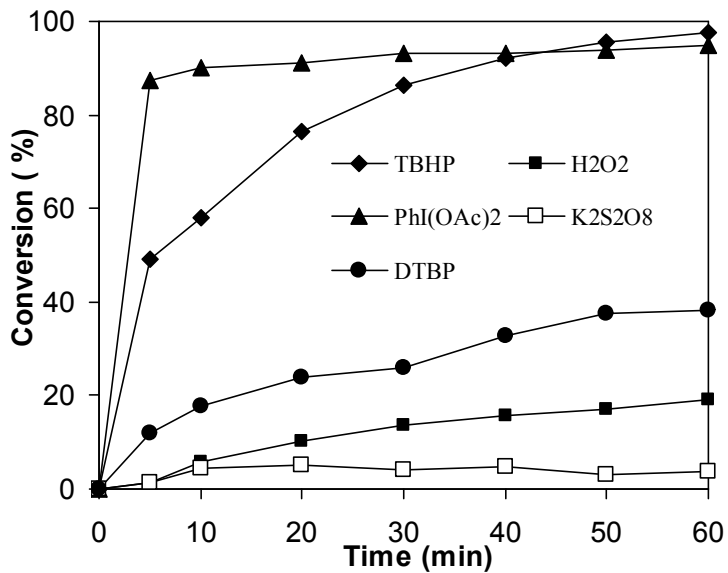


Fig. S16. Effect of different oxidants on reaction conversion.

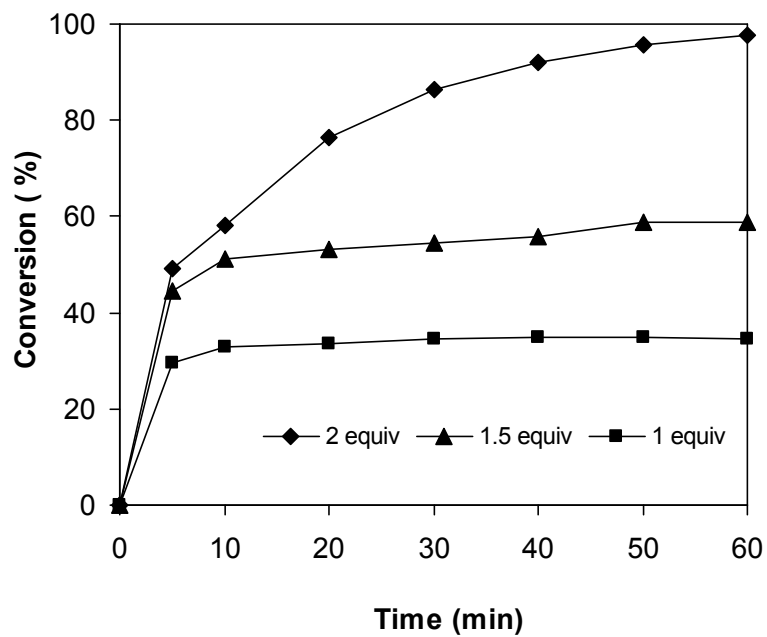


Fig. S17. Effect of *tert*-butyl hydroperoxide concentration on reaction conversion.

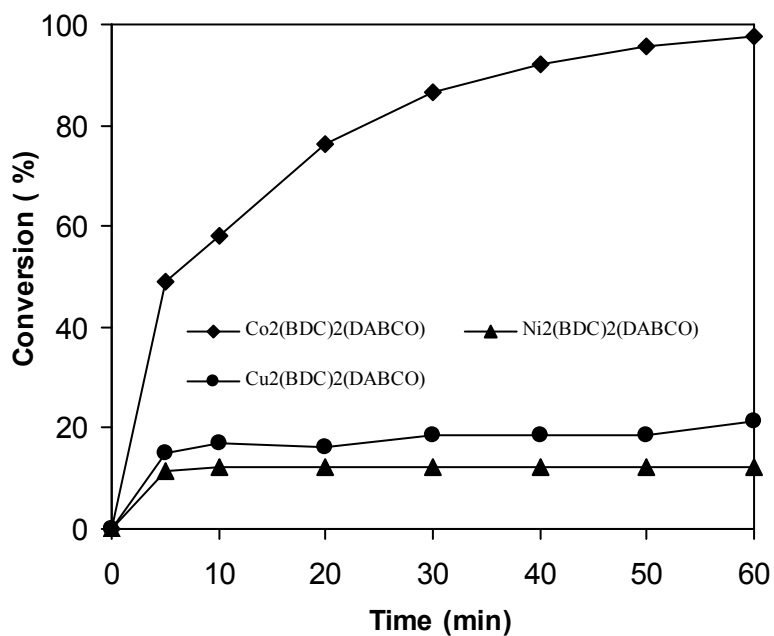


Fig. S18. Different MOFs as catalyst for the direct benzoxazole amination reaction.

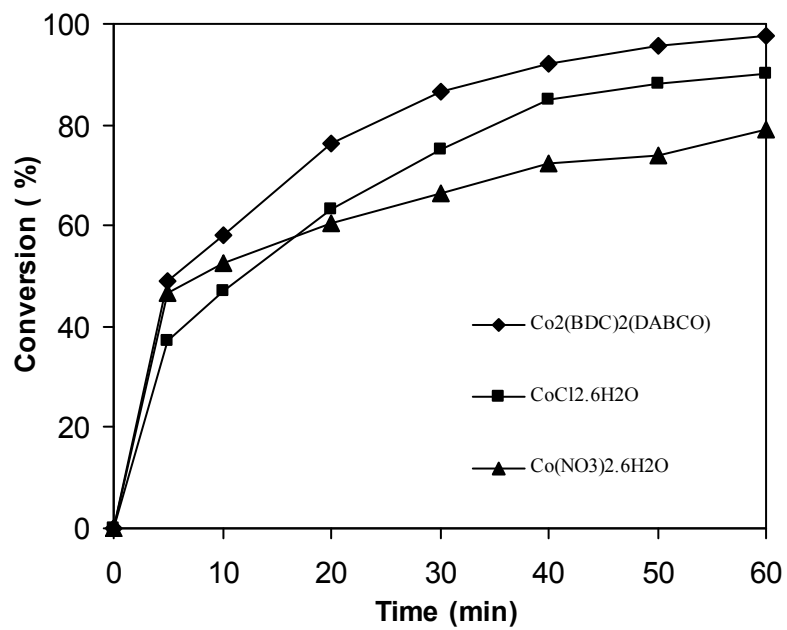


Fig. S19. Difference in activity between VNU-10 and cobalt salts as catalyst for the direct benzoxazole amination reaction.

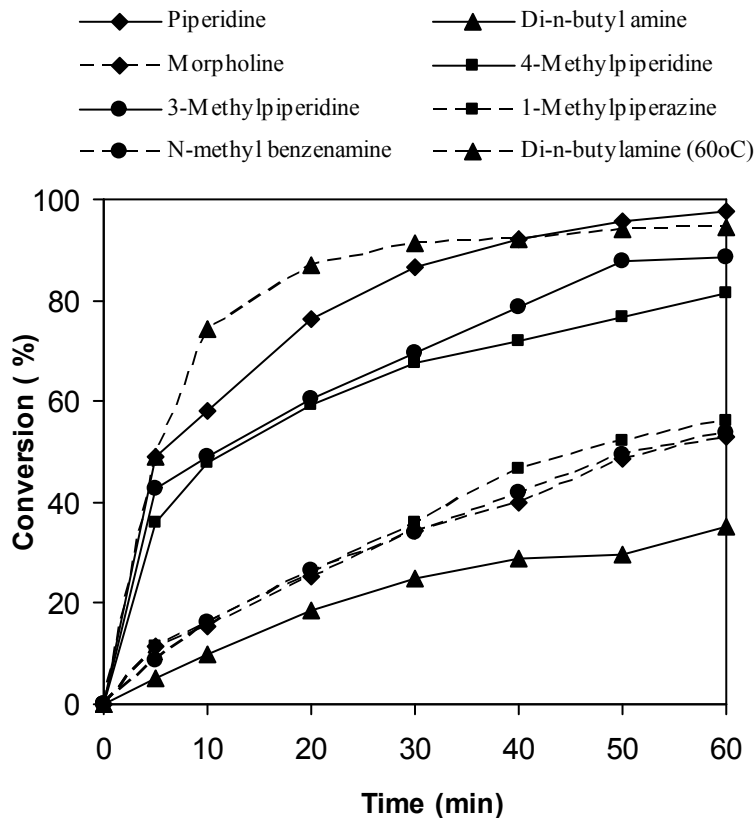


Fig. S20. Effect of different amines on reaction conversion.

### Reactions with different $\text{Co}_2(\text{BDC})_2(\text{DABCO})$ particle size

By conducting the synthesis procedure with longer time (24 hours in isothermal oven),  $\text{Co}_2(\text{BDC})_2(\text{DABCO})$  with larger particle size was obtained. Grinding with different level was carried out to form two  $\text{Co}_2(\text{BDC})_2(\text{DABCO})$  with smaller particle sizes (Fig. S21). Experiments using these  $\text{Co}_2(\text{BDC})_2(\text{DABCO})$  were performed under optimal conditions.

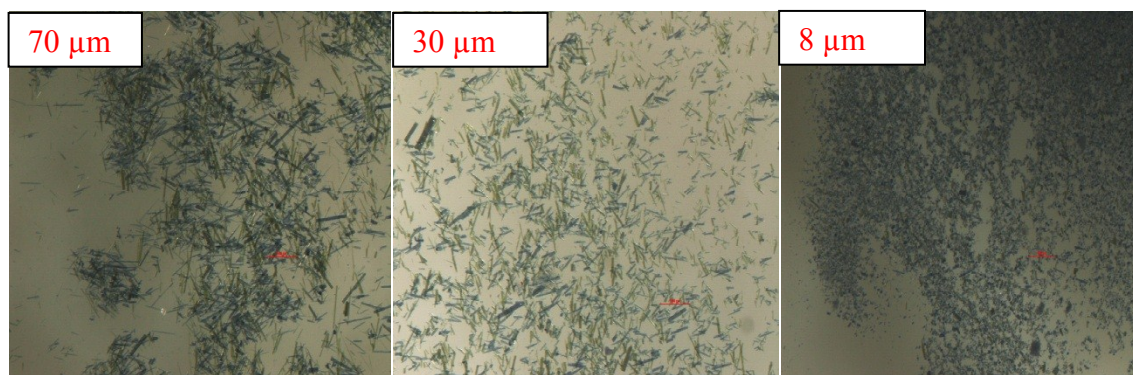


Fig. S21.  $\text{Co}_2(\text{BDC})_2(\text{DABCO})$  with different particle size

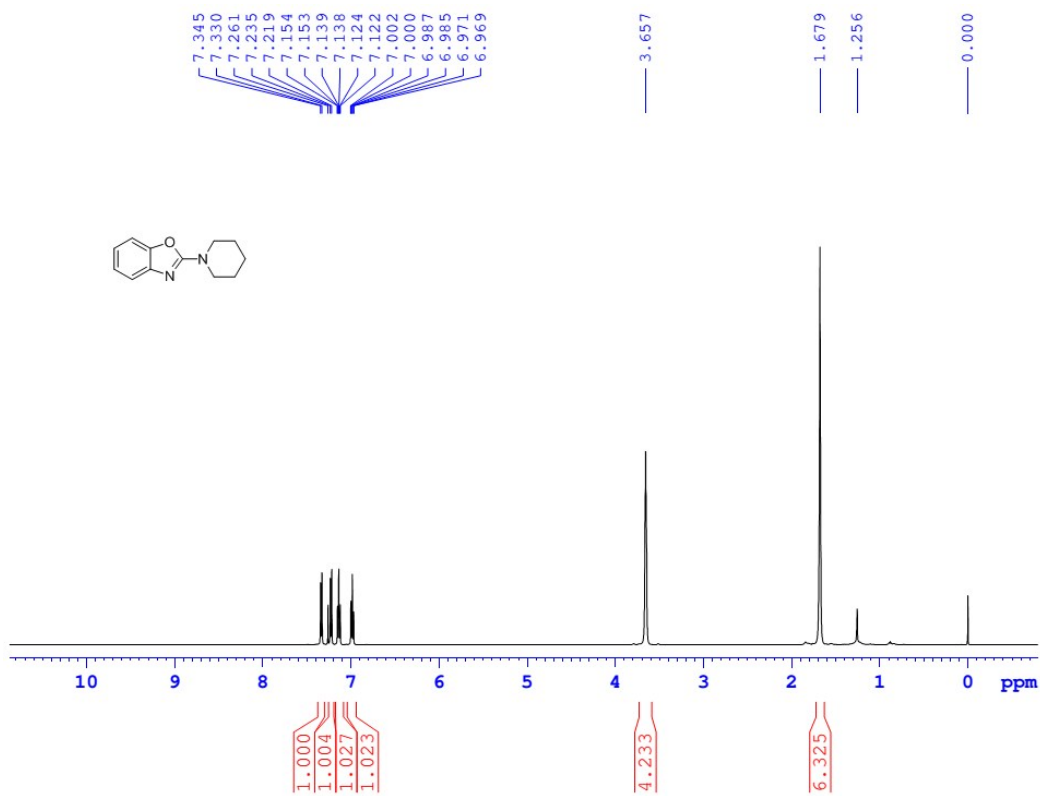


Fig. S22. Spectral Copies of  $^1\text{H}$  of 2-(piperidin-1-yl)benzoxazole



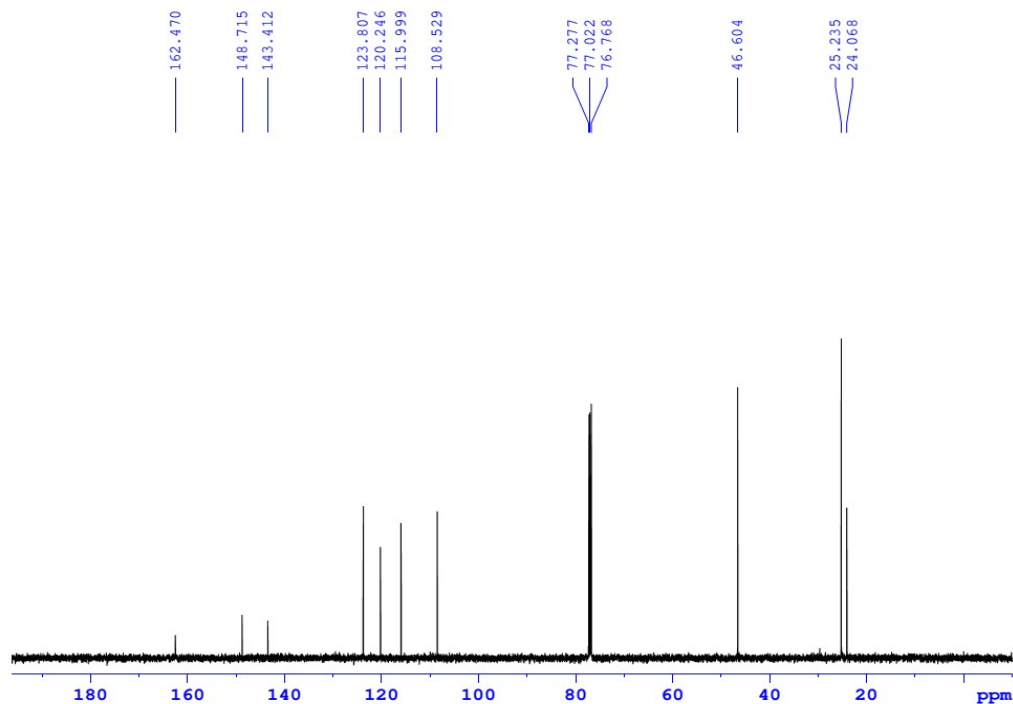


Fig. S23. Spectral Copies of  $^{13}\text{C}$  NMR of 2-(piperidin-1-yl)benzoxazole

### Characterization Data for Products

**2-(piperidin-1-yl)benzoxazole.** Prepared as shown in the general experimental procedure and purified on silica gel (EtOAc/hexane = 1:9): yellow solid; yield 86%.  $^1\text{H}$  NMR ( $\text{CDCl}_3$ , 500 MHz)  $\delta$ (ppm) 1.679 (s, 6H), 3.657 (s, 4H), 6.969 (t,  $J$ = 8.0 Hz, 1H), 7.122 (t,  $J$ = 8.0 Hz, 1H), 7.219 (d,  $J$ = 8 Hz, 1H), 7.330 (d,  $J$ =8 Hz, 1H);  $^{13}\text{C}$  NMR ( $\text{CDCl}_3$ , 125 MHz)  $\delta$ (ppm) 24.068, 25.235, 46.604, 108.529, 115.999, 120.246, 123.807, 143.421, 148.715, 162.470; GC-MS (EI)  $m/z$ = 202  $[\text{M}]^+$ .